Quantification of Residual Water in Pharmaceutical Frozen Solutions via ^{1}H Solid-state NMR

Yong Du and Yongchao Su*

Analytical Research and Development, Merck & Co., Inc., Rahway, NJ 07065, USA

*Corresponding author: Y.S.: yongchao.su@merck.com

https://doi.org/10.26434/chemrxiv-2023-mmxqx **ORCID:** https://orcid.org/0000-0001-5063-3218 Content not peer-reviewed by ChemRxiv. **License:** CC BY-NC-ND 4.0

Table of Content (TOC) Figure

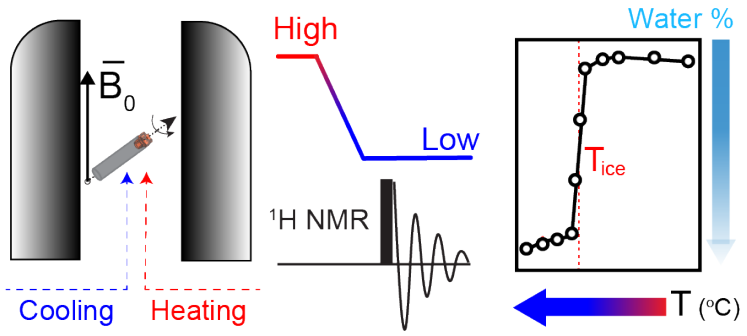

https://doi.org/10.26434/chemrxiv-2023-mmxqx **ORCID:** https://orcid.org/0000-0001-5063-3218 Content not peer-reviewed by ChemRxiv. **License:** CC BY-NC-ND 4.0

Abstract

Freezing is essential for the stability of biological drug substances and products, particularly in frozen solution formulations and during the primary drying of lyophilized preparations. However, the unfrozen segment within the frozen matrix can alter solute concentration, ionic strength, and stabilizer crystallization, posing risks of increased biophysical instability and faster chemical degradation. While quantifying the unfrozen water content is crucial for designing stable biopharmaceuticals, there is a lack of analytical techniques for in situ quantitative measurements. In this study, we introduce a ^{1}H magic angle spinning NMR technique to identify the freezing point (T_{ice}) and quantify mobile water content in frozen biologics. Our quantitative results demonstrate that water freezing is influenced by buffer salt properties and formulation composition, including the presence of sugar cryoprotectants and protein concentration. Additionally, the ^{1}H chemical shift can probe pH in the unfrozen phase, potentially predicting the microenvironmental acidity in the frozen state. Our proposed methodology provides fresh insights into the analysis of freeze-concentrated solutions, enhancing our understanding of the stability of frozen and lyophilized biopharmaceuticals.

https://doi.org/10.26434/chemrxiv-2023-mmxqx **ORCID:** https://orcid.org/0000-0001-5063-3218 Content not peer-reviewed by ChemRxiv. **License:** CC BY-NC-ND 4.0

1. Introduction

Freezing is routinely utilized to cool an aqueous solution below its freezing point, leading to its solidification. This process has a broad range of applications, from preserving biological samples, cells, embryos, to food, and more.[1, 2]. Within the pharmaceutical realm, frozen solutions play a pivotal role in two primary contexts. First, biopharmaceutical drug substances and products are frequently stored and transported in a frozen state to bolster their stability. Notably, commercial biotherapeutics, like the COVID-19 mRNA vaccines, are maintained in frozen conditions to address stability challenges and ensure potency. [1] Second, the fabrication of lyophilized dosages necessitates the employment of frozen solutions in the preliminary phase.[1, 3] Consequently, understanding the physicochemical properties of frozen matrices is paramount for developing biopharmaceutical products.

While the freezing process offers advantages, it also subjects materials to various stresses such as ice formation, pH shifts, and freeze concentration. These stresses can compromise the integrity of biological therapeutics, leading to denaturation, aggregation, and reduced bioactivity.[4] As freezing begins and the first ice nucleus emerges, a dual-phase system arises. This system encompasses a solid phase and a freeze-concentrated solution phase, where the majority of the water transforms into solid ice crystals.[5] Grasping the characteristics of the freeze-concentrate solution phase is vital because the stability and functionality of biologics are intimately tied to the unfrozen segment. For instance, numerous studies have shown that protein aggregation is notably precarious at the water-ice interface.[6] Upon freezing, protein molecules are often repelled from ice crystals, making them increasingly vulnerable to the chemical and physical alterations transpiring in the unfrozen section.[7] Moreover, as ice crystals grow, there's a rise in solute concentration and viscosity within the unfrozen phase. This enhanced molecular crowding can negatively impact protein stability.[8] Equally concerning is the pH shift within the freeze concentrate. This shift, caused by the selective crystallization of buffer components, can destabilize proteins.[9] Altogether, the stresses such as the water-ice interface, solute concentration, ionic strength, and stabilizer crystallization hinge on the quantity of unfrozen water present in the frozen solution.

The content of unfrozen water in frozen solutions plays a significant role in the lyophilization (or freeze-drying) process. Research has shown that the residual moisture content, which is partly retained from the unfrozen water during freeze-drying, profoundly influences the solid-state stability of biopharmaceutical products.[10] When residual moisture surpasses the monolayer hydration level, protein degradation can ensue. This is because the absorbed water becomes more mobile, inducing greater protein flexibility.[10] During lyophilization, primary drying eliminates ice from the frozen solution. In contrast, the secondary drying phase desorbs unfrozen water through the pores in the dried cake.[5] The volume of unfrozen water present in the frozen solution can directly influence secondary drying conditions. Excessive unfrozen water can extend the secondary drying phase, leading to elevated processing durations and energy expenditures. This can compromise the efficiency of the entire procedure. Therefore, precisely gauging the unfrozen water content in frozen solutions is vital, both for preserving sensitive biologics in a frozen state and for manufacturing stable freeze-dried products.

Differential scanning calorimetry (DSC) has been explored for its potential to ascertain the composition of freeze concentrates in frozen solutions.[11, 12] For instance, Friess and colleagues employed DSC techniques to probe the composition of maximally freeze-concentrated solutions, determining that 20-30% of the freeze concentrate comprised water. This percentage exhibited slight variations based on

https://doi.org/10.26434/chemrxiv-2023-mmxqx **ORCID:** https://orcid.org/0000-0001-5063-3218 Content not peer-reviewed by ChemRxiv. **License:** CC BY-NC-ND 4.0

buffering excipients.[12] However, the direct quantification of unfrozen water using DSC remains elusive. Earlier studies have leveraged nuclear magnetic resonance (NMR) to discern the amount of unfrozen water in frozen materials.[13-16] For example, Watanabe and Mizoguchi employed the T_2 relaxation method to gauge unfrozen water quantities in frozen porous glass powders, fujinomori soil, and bentonite.[17] Similarly, Lucas et al. assessed the ice content in frozen sucrose-protein solutions using a congruent approach.[14] In such T_2 relaxation-focused experiments, the free induction decay value is recorded and then fitted to deduce both liquid water and ice content within a specimen. Alternatively, other endeavors have harnessed deuterium NMR methodologies to approximate unfrozen water content in systems like frozen water–poly(vinyl alcohol), by analyzing the ^2H signal intensity of D_2O.[15] Dehl quantified the mobile water content in collagen by observing the broad-line NMR splitting of D_2O.[16]

The accurate measurement of unfrozen water content in frozen pharmaceutical formulations has not yet been reported. The absence of in situ analysis during the freezing complicates the monitoring of the water transition from its aqueous to frozen state. In this study, we introduce a novel technique utilizing magic angle spinning (MAS) ^1H NMR to quantify the unfrozen water content in frozen pharmaceutical compounds, closely observing ice crystallization at sub-zero temperatures. We also discerned that the ^1H chemical shift of water is sensitive to variations in pH and buffer concentrations. A pronounced correlation between 1H chemical shifts and the pH of the original solutions was detected. As a testament to the efficacy of our 1H ssNMR methodology, we successfully analyzed Dupixent®, a commercially available monoclonal antibody (mAb) formulation, precisely measuring its unfrozen water content in a frozen state.

2. Materials and Methods

2.1 Materials

Anhydrous trehalose, 1 N HCl, and methanol were purchased from Fisher Scientific. Anhydrous Na_2HPO_4 and NaH_2PO_4 were purchased from Sigma Aldrich. 1 N NaOH was purchased from J.T. Baker. Three types of solution were prepared in the current study: (1) sodium phosphate (NaP) buffer solutions with different buffer concentrations; (2) 100 mM NaP buffer solutions with different concentrations (% w/v) of trehalose; and (3) NaP buffer solutions (10, 20, 50, and 100 mM) with 5% w/v trehalose and pH values of 2, 5, and 7, respectively. To prepare these solutions, appropriate amounts of Na_2HPO_4, NaH_2PO_4, and trehalose powders were dissolved in 100 mL MilliQ water. The pH of the buffer solutions was then adjusted via titration with the HCl or NaOH solution and calibrated by a Mettler Toledo pH meter. Additionally, Dupixent® containing 150 mg/mL of dupilumab was purchased through Myonex, LLC (Norristown, PA). To test the effect of dupilumab concentration on the unfrozen water content, two more samples with 50 and 10 mg/mL of dupilumab were also prepared. In all ssNMR measurements, about 100 μL of the solution was filled into the 4 mm Zirconia rotor and sealed with the Vespel driving cap.

2.2 Solid-state Nuclear Magnetic Resonance Spectroscopy

All ssNMR experiments were carried out on a 9.4T Bruker AVANCE NEO spectrometer equipped with a 4 mm HXY probe tuned to $^1H/^{31}P/^{13}C$ triple resonances. All samples were spun at 3.5 kHz, except where specified. ^1H single pulse experiments were collected over a temperature range of 25 to -35°C. The ^1H 90° pulse was calibrated for all solution samples within the temperature range studied. The ^1H chemical shifts were externally referenced to the hydroxyl peak of water at 4.75 ppm at 25°C. All NMR data were processed using Bruker TopSpin.

https://doi.org/10.26434/chemrxiv-2023-mmxqx **ORCID:** https://orcid.org/0000-0001-5063-3218 Content not peer-reviewed by ChemRxiv. **License:** CC BY-NC-ND 4.0

3. Results and Discussion

3.1 *In situ* cooling for analyzing frozen solution

One of the goals of this study is to provide *in situ* analysis of frozen solutions. ssNMR has demonstrated capabilities of characterizing hydrated and phase-separated molecular systems at a broad range of temperatures.[18] **Figure 1** illustrates the scheme of *in situ* ssNMR experiments for studying the frozen solutions. The sample temperature was regulated by balancing the probe heating and cooling from SmartCooler BCU II (Bruker). The cooling rate was controlled at 1°C/min using the Slope Limited regulation mode provided in the Variable Temperature Unit in TopSpin software with an uncertainty of ± 1°C. ^{1}H single pulse experiments were carried out by allowing the temperature to stabilize for 30 minutes. Cooling using a typical BCU can achieve a temperature as low as -50°C. It has also been reported that the low-temperature probes in dynamic nuclear polarization (DNP) ssNMR experiments can routinely reach as cold as -173°C using nitrogen cooling gas.[19] This can sufficiently cover the temperature requirement in pharmaceutical applications, such as ultracold storage or deep freeze for Covid-19 vaccines requiring as low as -90°C.[19]

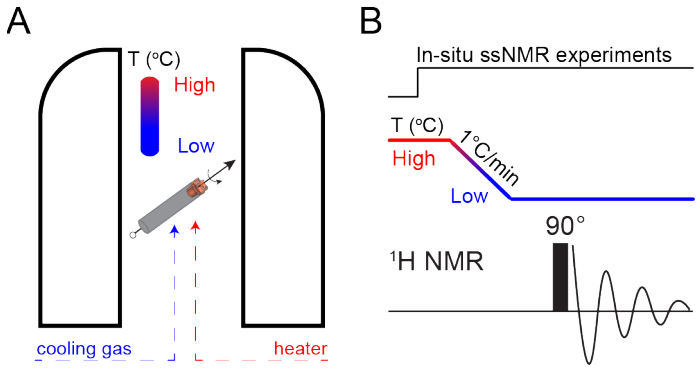

Figure 1. Schematic representation of *in situ* ssNMR characterization of a frozen solution. (A) Sample temperature control during spinning within the NMR magnet; and (B) ^{1}H single pulse experiment conducted at specific low temperatures. The study employs a lyophilization-relevant temperature range from 25°C to -35°C.

In ssNMR, the rotor was placed at the magic angle (i.e., 54.74°) with respect to the static field (B_0) and spun at a high frequency to improve the spectral resolution. However, the frictional heating produced by MAS can cause the sample temperature to deviate significantly from the nominal temperature. For instance, a temperature difference of up to 58°C was previously reported at 18 kHz MAS frequency.[20] Therefore, it is essential to accurately calibrate the actual sample temperature in the study of frozen solution. Previously, Thurber and Tycho approached this by using the chemical shifts and spin-lattice relaxation rate of KBr powder to measure the internal sample temperatures.[21] In our work, temperature calibration was carried out using methanol as an NMR thermometer, given its low freezing point of approximately -97.6°C.[22] The actual sample temperature can be determined using the ^{1}H chemical shift difference ($\Delta\delta$) between the methyl and hydroxy peaks of methanol, as derived by **Equation 1**.[22] This method can be used to calibrate the temperature within a range of approximately -95°C to 57°C, which is within its melting and boiling point, -97.6°C and 64.7°C, respectively.

$$T\ (°C) = 135.85 - 36.54 \times \Delta\delta - 21.85 \times (\Delta\delta)^2 \qquad \text{Eq. 1}$$

https://doi.org/10.26434/chemrxiv-2023-mmxqx **ORCID:** https://orcid.org/0000-0001-5063-3218 Content not peer-reviewed by ChemRxiv. **License:** CC BY-NC-ND 4.0

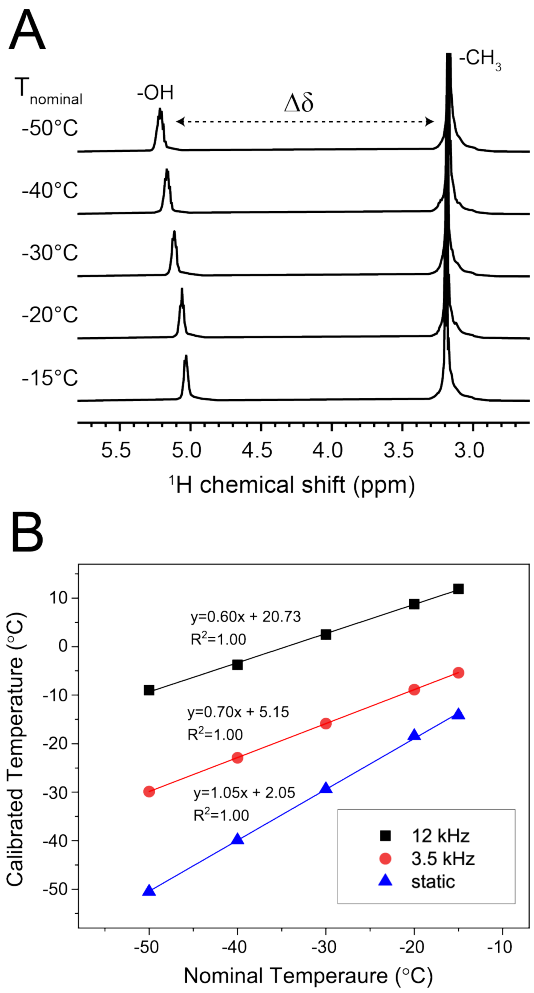

Figure 2. (A) 1D ^{1}H NMR spectra of methanol at various nominal temperatures, acquired at a MAS rate of 3.5 kHz; and (B) Temperature calibration curves corresponding to MAS frequencies of 12, 3.5, and 0 kHz. Sample temperatures are maintained with a probe cooling gas flow of 1200 lph.

Figure 2A demonstrates the ^{1}H ssNMR spectra of methanol obtained at different nominal (or thermocouple-reported) temperatures with a MAS frequency of 3.5 kHz and a cooling gas flow rate of 1200 liter per hour (lph). The hydroxyl peak gradually shifts downfield as the temperature decreases, while the chemical shift of the methyl peak remains the same. The difference in chemical shift between the methyl and hydroxyl peaks is utilized to determine the actual temperature. **Figure 2B** plots the correlation of actual (or calibrated) and nominal temperatures at three different spinning rates, 0 kHz (blue), 3.5 kHz (red), and 12 kHz (black). The actual sample temperatures are expected to be identical to the nominal temperatures without spinning. In contrast, at 12 kHz of MAS, the frictional heating results in significant temperature deviations, with an observed temperature difference of up to 40°C. This frictional heating is significantly reduced when the MAS rate is reduced to 3.5 kHz, enabling actual temperatures of -5 to -30°C to be achieved when nominal temperatures are set at -15 to -50°C, respectively. Additionally, sample frictional heating is influenced by the cooling gas flow rate. A similar temperature calibration was conducted with a 500 lph flow rate of cooling gas, and the results are summarized in **Figure S1**. One interesting observation in **Figure S1B** is that at higher nominal temperatures (>25°C), the actual temperatures under 3.5 kHz of MAS are lower than those under static conditions. This implies that the cooling effect from driving and

https://doi.org/10.26434/chemrxiv-2023-mmxqx **ORCID:** https://orcid.org/0000-0001-5063-3218 Content not peer-reviewed by ChemRxiv. **License:** CC BY-NC-ND 4.0

bearing gases on the sample temperature is more significant than the frictional heating from the spinning at 3.5 kHz.

3.2 Quantification of unfrozen water in frozen solutions

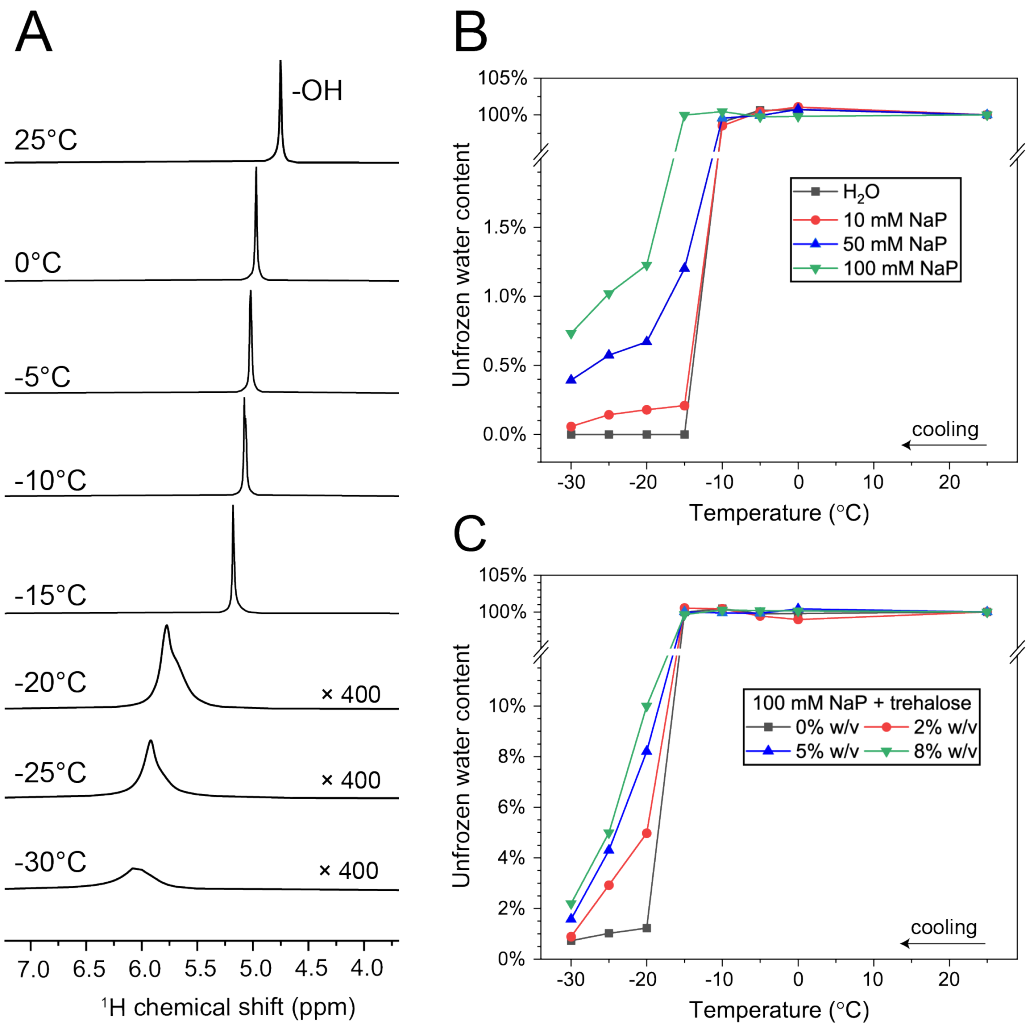

Figure 3. (A) 1D ^{1}H NMR spectra of 100 mM NaP buffer during an *in situ* freezing process ranging from 25°C to -30°C, with all spectra acquired at a MAS frequency of 3.5 kHz. Illustration of the effects of buffer (B) and trehalose (C) on the unfrozen water content in the phosphate-buffered frozen solutions.

The freezing process can be segmented into three distinct stages. Initially, during the cooling phase, the aqueous solution is brought down from its starting temperature to the point where ice crystals begin to form. This leads to the phase change stage, where subsequent to the initiation of the first ice nucleus, ice crystals continue to grow. The process culminates in the solidification stage, where ice crystal growth reaches its limit, and no further growth occurs.[5] It's worth noting that the amount of unfrozen water present in freeze-concentrate can profoundly influence vital parameters like the ice-aqueous interfacial area, solute concentration levels, and both primary and secondary drying rates during freeze-drying. Consequently, obtaining quantitative data on this unfrozen water content is pivotal in grasping the mechanisms behind

https://doi.org/10.26434/chemrxiv-2023-mmxqx **ORCID:** https://orcid.org/0000-0001-5063-3218 Content not peer-reviewed by ChemRxiv. **License:** CC BY-NC-ND 4.0

protein denaturation throughout the freeze-thaw and freeze-drying cycles. NMR stands out as a quantitatively robust technique, given that its signal intensity directly correlates with the number of nuclei present, allowing for the absolute quantification of substances using both internal and external standards.[23] Specifically, ^{1}H NMR presents a promising methodology for quantifying unfrozen water, capitalizing on the pronounced linewidth variations between unfrozen water and ice. The spin-spin relaxation rate, R_2, for ice, is roughly 10^6 s^{-1}, leading to a notably broader ice signal than liquid water.[24] Furthermore, the ^{1}H signal of ice is exceptionally faint due to its prolonged longitudinal relaxation time, hovering around 1000 s.[25] As a result, the lingering and expansive ^{1}H peak of ice is anticipated to be barely distinguishable from baseline noise.

Figure 3A includes the ^{1}H NMR spectra of a 100 mM NaP buffer (pH 7.0) acquired at varying temperatures during freezing. In this study, the spectral integration of the H_2O signal was utilized to indicate the quantity of unfrozen water within the sample. To determine the content of unfrozen water at different temperatures, the peak integration of the hydroxyl peak was normalized against the value recorded at 25°C. Notably, NMR spin polarizations at thermal equilibrium display an inverse relationship with temperature. This relationship is accounted for when calculating the unfrozen water content.[26] Additionally, It is worth noting that the recycle delays in all ^{1}H experiments were sufficiently extended to ensure complete longitudinal relaxation. Interestingly, the total water content remains constant as temperature decreases during the cooling stage (25℃ to a point between -15 and -20℃). The data demonstrates that the 100 mM NaP buffer does not freeze spontaneously at its equilibrium freezing temperature (~0°C). Instead, the aqueous system supercools and remains liquid below -15°C. The degree of supercooling, defined as the difference between ice formation temperature (T_{ice}) and equilibrium freezing temperature, is roughly -15 to -20°C. The degree of supercooling directly impacts the size, number, and morphology of ice crystals that form during freezing, which influences the subsequent drying process in lyophilization, for example, the resistance to water vapor flow.[5] Therefore, precise measurement and control of the degree of supercooling is crucial for developing effective and consistent freeze-drying processes. Moreover, the hydroxyl peak linewidth of unfrozen water increases with decreasing temperature, suggesting the loss of mobility of the unfrozen phase in frozen solution.[27]

Moreover, **Figure 3B** illustrates the correlation between unfrozen water content and temperature for pure water and NaP buffers at three concentrations: 10, 50, and 100 mM. For ease of signal intensity comparison, hydroxyl signal intensities from aqueous solutions at 25℃ serve as the baseline, assigned a value of 100% on the ordinate axis. At -20℃, the unfrozen water content in the 100 mM NaP buffer drops to just under 1.5%. As the cooling progresses, this content further diminishes, settling at around 0.7% at -30℃. This reduction is attributed to the ongoing growth of ice crystals in the frozen mixture. This observation aligns with findings by Volke et al., who estimated unfrozen water content in frozen protein solutions to be between 0.56-0.8% at 248 K.[28] Interestingly, the freezing temperature, T_{ice}, is influenced by the buffer concentration. Specifically, a 100 mM NaP buffer shows a lower T_{ice} compared to pure water and 10 and 50 mM NaP buffer solutions. This trend is consistent with the anticipated freezing point depression in water due to increased buffer concentration. Furthermore, these results indicate the interdependence of unfrozen water content on both freezing temperature and buffer concentration. At equivalent temperatures, higher buffer concentrations yielded greater unfrozen water content.

https://doi.org/10.26434/chemrxiv-2023-mmxqx **ORCID:** https://orcid.org/0000-0001-5063-3218 Content not peer-reviewed by ChemRxiv. **License:** CC BY-NC-ND 4.0

Sugar molecules, such as sucrose and trehalose, are commonly utilized as cryoprotectants in pharmaceutical formulations. In this context, we examined the impact of trehalose on the unfrozen water content during freezing, with findings illustrated in **Figure 3C**. Interestingly, introducing trehalose elevates the unfrozen water content in frozen NaP buffer (100 mM) solutions relative to the unadulterated buffer. Our methodology not only facilitates the real-time quantification of unfrozen water but also affords meticulous control over various determinants in the freezing process, including the cooling rate and annealing duration. Previous research has highlighted the cooling rate's role in determining ice crystal size during freezing: faster cooling rates typically yield smaller ice crystals.[29] To delve further into this aspect, our study explored how different cooling rates affected the amount of unfrozen water in the frozen matrix. **Figure S2** showcases the unfrozen water content in a 100 mM NaP buffer subjected to two distinct cooling rates: 1°C/min and 5°C/min. Notably, while an elevated cooling rate advances the freezing point (T_{ice}), the unfrozen water content was found to be generally consistent across both cooling rates when observed between -20 to -30°C.

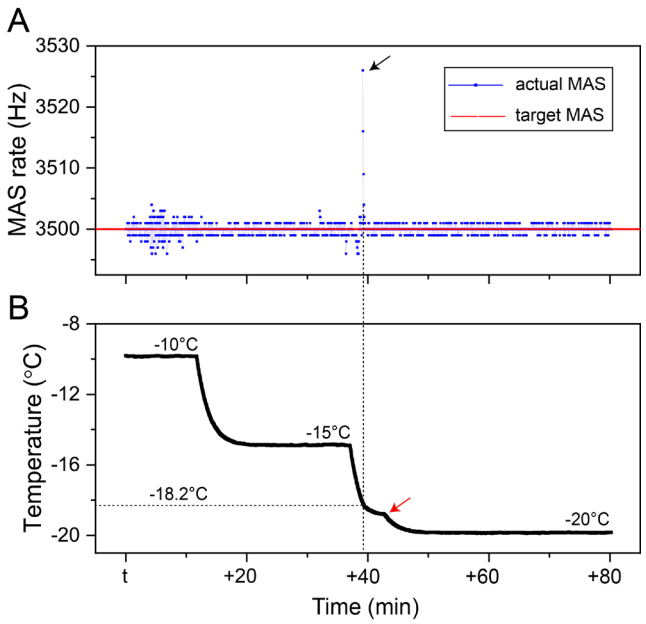

Figure 4. Freezing process of 100 mM NaP buffer containing 2% w/v trehalose as probed by MAS rate (A) and nominal sample temperature (B) during cooling from -10°C to -20°C. The target MAS is set at 3.5 kHz. Black and red arrows respectively denote the time points for ice formation and exothermic events observed during water freezing.

The data in **Figure 3** indicate that the freezing point of the buffer system can be approximated within a 5°C span. We also employed alternative techniques to identify ice formation with greater precision. **Figure 4A** showcases the MAS profile for the 100 mM NaP buffer enriched with 2% w/v trehalose. As temperatures shift between -10 and -20°C, the MAS rate consistently holds at 3.5 kHz. However, an abrupt shift of roughly 30 Hz in the MAS is evident at -18.2°C (as pointed out by the black arrow in **Figure 4A**). Interestingly, this MAS shift corresponds directly with the temperature change highlighted in **Figure 4B**. The act of ice formation is characterized by an exothermic release. This energy discharge (marked by the red arrow in **Figure 4B**) impacts the initial cooling trajectory between -15 to -20°C, resulting in a

https://doi.org/10.26434/chemrxiv-2023-mmxqx **ORCID:** https://orcid.org/0000-0001-5063-3218 Content not peer-reviewed by ChemRxiv. **License:** CC BY-NC-ND 4.0

discernible delay or modification. Overall, these observations underscore the potential of ssNMR to investigate thermal phenomena, like the onset of ice formation, with remarkable sensitivity.

3.3 Correlation of water chemical shift and pH in frozen solutions

Freezing an aqueous solution can lead to the potential crystallization of buffer components, which may be coupled with pH alterations and elevated ionic strength.[12] It's essential to understand these stress-triggered changes in physiochemical properties, as this knowledge can enhance the process development of biopharmaceuticals during freezing. NMR chemical shifts are sensitive to varying chemical and physical conditions. In particular, ^{1}H NMR chemical shifts have proven instrumental in determining solution pH values, molecular pKa values, chemical kinetics, and solution temperatures.[22, 30] As an illustration, the ^{1}H chemical shift of water in a solution is contingent upon the temperature, characterized by a coefficient of -11.9 ± 0.3 ppb/°C.[31] Other factors, like pH and salt concentration, are also known to influence the water chemical shift.[31] In our current study, we delved deeper into understanding how the ^{1}H chemical shifts of unfrozen water change based on the pH of the original solution. **Figure 5A** displays the ^{1}H spectra for 50 mM NaP buffer solutions with 5% w/v trehalose at -25°C across various pH levels. The addition of trehalose mitigates the pH shift observed in NaP buffer, resulting from the selective crystallization of Na_2HPO_4 into $Na_2HPO_4{\cdot}12H_2O$.[32] It was postulated that the frozen NaP buffer, even at reduced temperatures, would maintain a pH closely resembling its original solution. As highlighted in **Figure 5A**, the hydroxyl peak of the unfrozen water exhibits a systematic downfield shift as the pH reduces. **Figure 5B** delineates the relationship between the hydroxyl peak chemical shift and the initial pH of solutions for NaP buffers of concentrations 10, 20, 50, and 100 mM at -25°C. Interestingly, the slope for the 10 mM buffers stands out for its pronounced steepness, especially in comparison to the 50 and 100 mM NaP buffers. Further examinations showcasing the link between the hydroxyl peak chemical shift and pH for these buffer solutions at temperatures of -20 and -30°C can be found in **Figure S3**.

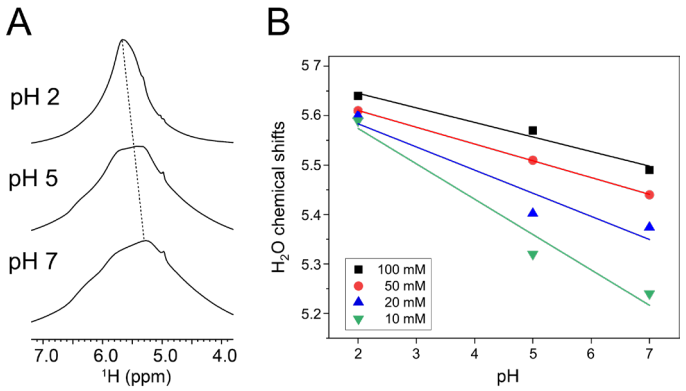

Figure 4. (A) 1D ^{1}H NMR spectra of 50 mM NaP frozen solutions containing 5% w/v trehalose at -25°C, showcasing variations with different initial pH values; and (B) the correlation between the ^{1}H chemical shift of unfrozen water and pH for NaP buffer solutions at concentrations of 10, 20, 50, and 100 mM at -25°C.

The relationship between chemical shift and pH was observed to be influenced by the concentration of NaP buffer in its frozen state, as shown in **Figure S4**. Specifically, there is a swift change in the chemical shift-pH slope at lower buffer concentrations, but it stabilizes and approaches a plateau as the concentration increases. This indicates that the buffer concentration in the unfrozen phase has a significant role in

https://doi.org/10.26434/chemrxiv-2023-mmxqx **ORCID:** https://orcid.org/0000-0001-5063-3218 Content not peer-reviewed by ChemRxiv. **License:** CC BY-NC-ND 4.0

adjusting the water's chemical shift, not just the effects of pH. This phenomenon indicates the influence of phosphate buffer concentration on apparent pK_{a2}, as illustrated in **Figure S5**.[33] Here, the apparent pK_{a2} experiences a sharp decline with rising NaP concentration and slowly stabilizes upon reaching a higher concentration plateau, typically in the range of 0.5-1.0 M. Moreover, as the temperature decreases, the concentration threshold for this slope plateau shifts upwards incrementally.

3.4 Quantification of unfrozen water in frozen monoclonal antibody formulations.

Many biopharmaceutical drugs are stored in a frozen state for the cold chain supply. It has been reported that the water-ice interface and protein concentration can have a significant impact on the stability and bioactivity of protein formulations.[34, 35] For instance, Gonnelli and coworkers observed loss of stability of the azurin mutant C112S from *Pseudomonas aeruginosa* in ice, and the destabilization effect depends primarily on the size of the liquid water pool in equilibrium with ice, suggesting that water-ice interfacial stress is a controlling factor for protein instability.[36] In addition, Hauptmann et al. investigated the effect of protein concentration on the stability of a mAb during freeze-thawing and found that higher concentrations led to increased aggregation.[34] However, there is a lack of understanding regarding the correlation between unfrozen water content and protein concentration in frozen solutions. For this reason, we further explored the applicability of ^{1}H ssNMR methods in determining the unfrozen water content in a commercial mAb formulation, Dupixent®.

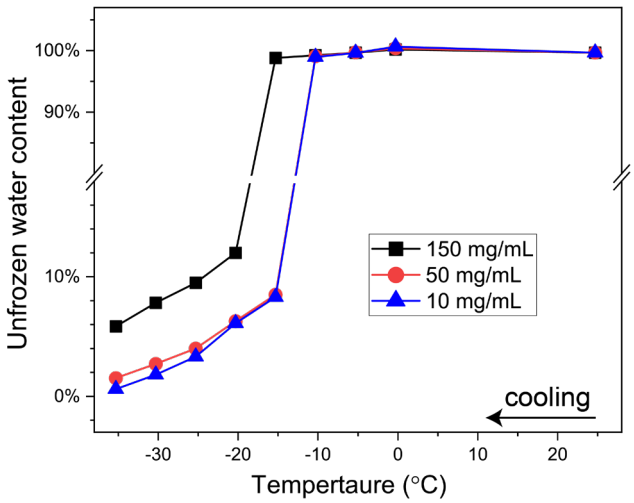

Figure 6. Quantification of unfrozen water in Dupixent® formulations represented by different concentrations of dupilumab: 150 mg/mL, 50 mg/mL, and 10 mg/mL.

Figure S6 presents the ^{1}H NMR spectra of Dupixent® drug products, each diluted to different concentrations (150, 50, and 10 mg/mL) of dupilumab. The unfrozen water content for each concentration is illustrated in **Figure 6** and varies with dupilumab concentration. Specifically, higher dupilumab concentrations yield increased unfrozen water levels in the frozen state. Additionally, the concentration directly affects the formulation's freezing point. For example, the original Dupixent® formulation (containing 150 mg/mL of dupilumab) began ice formation between -15 to -20°C. In contrast, the 50 and 10 mg/mL formulations started at slightly warmer ranges, between -10 to -15°C. The original Dupixent® formulation saw a significant drop in unfrozen water content to around 6% at 150 mg/mL dupilumab concentration. Meanwhile, the 50 and 10 mg/mL formulations had only approximately 2% and 1% unfrozen

https://doi.org/10.26434/chemrxiv-2023-mmxqx **ORCID:** https://orcid.org/0000-0001-5063-3218 Content not peer-reviewed by ChemRxiv. **License:** CC BY-NC-ND 4.0

water content, respectively, at the same temperature. These observations suggest a clear relationship between the mAb concentration and unfrozen water content in the frozen state. We hypothesize that higher mAb concentrations lead to correspondingly increased levels of unfrozen water when frozen. During freezing, solute molecules, such as mAb, are forced out of the forming ice crystals, leading to their accumulation in the residual liquid phase.[37] The intensity of this solute exclusion effect seems contingent on the mAb concentration in the solution. At diluted mAb concentrations, there's a lesser solute exclusion, permitting more water to join the ice crystals and thus resulting in lower unfrozen water content. Conversely, in more concentrated mAb solutions, a significant volume of mAb molecules is expelled from the crystallizing ice. This creates a need for a more significant amount of unfrozen water to sustain these displaced solutes.

The current study introduces an *in situ* method to quantify residual water in its frozen state. Such a measurement is of significant importance for several reasons. Unfrozen water acts as an active component in frozen solutions, partaking in chemical reactions and degradation processes during freeze storage.[38] It can also function as a solvent, facilitating the dissolution and interaction of various molecules in the freeze concentrate. This is concerning, as reactive entities in the freeze-concentrate can initiate chemical reactions harmful to biopharmaceuticals. Strambini and Gabellieri have shown that water solidification can profoundly alter protein structures, potentially due to the protein's direct interaction with ice.[39] Thus, assessing the quantity of unfrozen water is vital for grasping the instability risks tied to water-ice interfaces, ionic strengths, and solute concentrations.[3] Moreover, quantifying unfrozen water can provide a scientific basis for setting optimal temperatures for efficient manufacturing and cold chain distribution. This is crucial, considering the extensive vaccine wastage reported globally, primarily attributed to temperature deviations from recommended storage limits.[40] Furthermore, during the freeze-drying phase, the unfrozen water is eliminated through a desorption procedure of secondary drying. As a result, determining unfrozen water amounts is crucial for optimizing freezing and the subsequent drying processes in lyophile production.[5]

4. Conclusion

In summary, this study introduced an *in situ* ^{1}H MAS NMR technique to measure the unfrozen water content within frozen solutions. Our findings reveal that, quantitatively, water freezing depends on the physiochemical properties of buffer salts, such as pH and concentration, as well as formulation composition (e.g., the inclusion of sugar cryoprotectants and protein concentration). Moreover, the ^{1}H chemical shift of this unfrozen water robustly correlates with the pH of the original solutions. This research highlights the potential of ^{1}H ssNMR techniques in determining unfrozen water content in frozen biotherapeutics, offering valuable insights into their stability. We anticipate that the ^{1}H ssNMR approach will be promising for exploring a wide array of frozen pharmaceutical formulations across various freezing procedures.

5. Acknowledgement

Yong Du wishes to express gratitude to the Postdoctoral Program of Merck Sharp & Dohme LLC, a subsidiary of Merck & Co., Inc., located in Rahway, NJ, USA. We also extend our appreciation to our colleagues, including Drs. Ashley Lay-Fortenbery, Gennady Khirich, Donna M. Williams, Wei Xu, and Douglas D. Richardson, for their invaluable scientific discussions

6. Reference

https://doi.org/10.26434/chemrxiv-2023-mmxqx **ORCID:** https://orcid.org/0000-0001-5063-3218 Content not peer-reviewed by ChemRxiv. **License:** CC BY-NC-ND 4.0

(1) Authelin, J. R.; Rodrigues, M. A.; Tchessalov, S.; Singh, S. K.; McCoy, T.; Wang, S.; Shalaev, E. Freezing of Biologicals Revisited: Scale, Stability, Excipients, and Degradation Stresses. *J Pharm Sci* **2020**, *109* (1), 44-61. DOI: 10.1016/j.xphs.2019.10.062.
(2) Jang, T. H.; Park, S. C.; Yang, J. H.; Kim, J. Y.; Seok, J. H.; Park, U. S.; Choi, C. W.; Lee, S. R.; Han, J. Cryopreservation and its clinical applications. *Integrative Medicine Research* **2017**, *6* (1), 12-18. DOI: https://doi.org/10.1016/j.imr.2016.12.001. George, R. M. Freezing proceseses used in the food industry. *Trends in Food Science & Technology* **1993**, *4* (5), 134-138. DOI: https://doi.org/10.1016/0924-2244(93)90032-6.
(3) Bhatnagar, B. S.; Bogner, R. H.; Pikal, M. J. Protein Stability During Freezing: Separation of Stresses and Mechanisms of Protein Stabilization. *Pharmaceutical Development and Technology* **2007**, *12* (5), 505-523. DOI: 10.1080/10837450701481157.
(4) Bhatnagar, B. S.; Pikal, M. J.; Bogner, R. H. Study of the individual contributions of ice formation and freeze-concentration on isothermal stability of lactate dehydrogenase during freezing. *J Pharm Sci* **2008**, *97* (2), 798-814. DOI: 10.1002/jps.21017.
(5) Assegehegn, G.; Brito-de la Fuente, E.; Franco, J. M.; Gallegos, C. The Importance of Understanding the Freezing Step and Its Impact on Freeze-Drying Process Performance. *J Pharm Sci* **2019**, *108* (4), 1378-1395. DOI: 10.1016/j.xphs.2018.11.039.
(6) Fang, R.; Bogner, R. H.; Nail, S. L.; Pikal, M. J. Stability of Freeze-Dried Protein Formulations: Contributions of Ice Nucleation Temperature and Residence Time in the Freeze-Concentrate. *J Pharm Sci* **2020**, *109* (6), 1896-1904. DOI: 10.1016/j.xphs.2020.02.014. Tang, X.; Pikal, M. J. Design of Freeze-Drying Processes for Pharmaceuticals: Practical Advice. *Pharmaceutical Research* **2004**, *21* (2), 191-200. DOI: 10.1023/B:PHAM.0000016234.73023.75.
(7) Arakawa, T.; Prestrelski, S. J.; Kenney, W. C.; Carpenter, J. F. Factors affecting short-term and long-term stabilities of proteins. *Advanced Drug Delivery Reviews* **2001**, *46* (1), 307-326. DOI: https://doi.org/10.1016/S0169-409X(00)00144-7.
(8) Wang, Y.; Sarkar, M.; Smith, A. E.; Krois, A. S.; Pielak, G. J. Macromolecular crowding and protein stability. *J Am Chem Soc* **2012**, *134* (40), 16614-16618. DOI: 10.1021/ja305300m.
(9) Zbacnik, T. J.; Holcomb, R. E.; Katayama, D. S.; Murphy, B. M.; Payne, R. W.; Coccaro, R. C.; Evans, G. J.; Matsuura, J. E.; Henry, C. S.; Manning, M. C. Role of Buffers in Protein Formulations. *J Pharm Sci* **2017**, *106* (3), 713-733. DOI: 10.1016/j.xphs.2016.11.014. Kolhe, P.; Amend, E.; Singh, S. K. Impact of freezing on pH of buffered solutions and consequences for monoclonal antibody aggregation. *Biotechnology Progress* **2010**, *26* (3), 727-733, Article. DOI: 10.1002/btpr.377 Scopus.
(10) Towns, J. K. Moisture content in proteins: its effects and measurement. *Journal of Chromatography A* **1995**, *705* (1), 115-127. DOI: https://doi.org/10.1016/0021-9673(94)01257-F.
(11) Bhatnagar, B. S.; Cardon, S.; Pikal, M. J.; Bogner, R. H. Reliable determination of freeze-concentration using DSC. *Thermochimica Acta* **2005**, *425* (1), 149-163. DOI: https://doi.org/10.1016/j.tca.2004.06.017.
(12) Seifert, I.; Bregolin, A.; Fissore, D.; Friess, W. Method development and analysis of the water content of the maximally freeze concentrated solution suitable for protein lyophilisation. *Eur J Pharm Biopharm* **2020**, *153*, 36-42. DOI: 10.1016/j.ejpb.2020.05.027.
(13) Watanabe, K.; Wake, T. Measurement of unfrozen water content and relative permittivity of frozen unsaturated soil using NMR and TDR. *Cold Regions Science and Technology* **2009**, *59* (1), 34-41. DOI: 10.1016/j.coldregions.2009.05.011.
(14) Lucas, T.; Mariette, F.; Dominiawsyk, S.; Le Ray, D. Water, ice and sucrose behavior in frozen sucrose–protein solutions as studied by 1H NMR. *Food Chemistry* **2004**, *84* (1), 77-89. DOI: 10.1016/s0308-8146(03)00177-8.
(15) Gusev, D. G.; Lozinsky, V. I.; Vainerman, E. S.; Bakhmutov, V. I. Study of the frozen water–poly(vinyl alcohol) system by 2H and 13C NMR spectroscopy. *Magnetic Resonance in Chemistry* **1990**, *28* (7), 651-655, https://doi.org/10.1002/mrc.1260280717. DOI: https://doi.org/10.1002/mrc.1260280717 (acccessed 2022/10/28).

https://doi.org/10.26434/chemrxiv-2023-mmxqx **ORCID:** https://orcid.org/0000-0001-5063-3218 Content not peer-reviewed by ChemRxiv. **License:** CC BY-NC-ND 4.0

(16) Dehl, R. E. Collagen: Mobile Water Content of Frozen Fibers. *Science* **1970**, *170* (3959), 738-739. DOI: 10.1126/science.170.3959.738 (acccessed 2022/10/28).
(17) Watanabe, K.; Mizoguchi, M. Amount of unfrozen water in frozen porous media saturated with solution. *Cold Regions Science and Technology* **2002**, *34* (2), 103-110. DOI: https://doi.org/10.1016/S0165-232X(01)00063-5.
(18) Reif, B.; Ashbrook, S. E.; Emsley, L.; Hong, M. Solid-state NMR spectroscopy. *Nat Rev Methods Primers* **2021**, *1*. DOI: 10.1038/s43586-020-00002-1.
(19) Su, Y.; Andreas, L.; Griffin, R. G. Magic angle spinning NMR of proteins: high-frequency dynamic nuclear polarization and (1)H detection. *Annu Rev Biochem* **2015**, *84*, 465-497. DOI: 10.1146/annurev-biochem-060614-034206.
(20) Brus, J. Heating of samples induced by fast magic-angle spinning. *Solid State Nuclear Magnetic Resonance* **2000**, *16* (3), 151-160. DOI: https://doi.org/10.1016/S0926-2040(00)00061-8.
(21) Thurber, K. R.; Tycko, R. Measurement of sample temperatures under magic-angle spinning from the chemical shift and spin-lattice relaxation rate of 79Br in KBr powder. *J Magn Reson* **2009**, *196* (1), 84-87. DOI: 10.1016/j.jmr.2008.09.019.
(22) Ammann, C.; Meier, P.; Merbach, A. A simple multinuclear NMR thermometer. *Journal of Magnetic Resonance (1969)* **1982**, *46* (2), 319-321. DOI: https://doi.org/10.1016/0022-2364(82)90147-0.
(23) Holzgrabe, U.; Deubner, R.; Schollmayer, C.; Waibel, B. Quantitative NMR spectroscopy—Applications in drug analysis. *Journal of Pharmaceutical and Biomedical Analysis* **2005**, *38* (5), 806-812. DOI: https://doi.org/10.1016/j.jpba.2005.01.050.
(24) Siemer, A. B.; Huang, K. Y.; McDermott, A. E. Protein-ice interaction of an antifreeze protein observed with solid-state NMR. *Proc Natl Acad Sci U S A* **2010**, *107* (41), 17580-17585. DOI: 10.1073/pnas.1009369107.
(25) Bauer, T.; Gath, J.; Hunkeler, A.; Ernst, M.; Bockmann, A.; Meier, B. H. Hexagonal ice in pure water and biological NMR samples. *J Biomol NMR* **2017**, *67* (1), 15-22. DOI: 10.1007/s10858-016-0080-7.
(26) Sparrman, T.; Öquist, M.; Klemedtsson, L.; Schleucher, J.; Nilsson, M. Quantifying Unfrozen Water in Frozen Soil by High-Field 2H NMR. *Environmental Science & Technology* **2004**, *38* (20), 5420-5425. DOI: 10.1021/es0493695. Tycko, R. NMR at Low and Ultralow Temperatures. *Accounts of Chemical Research* **2013**, *46* (9), 1923-1932. DOI: 10.1021/ar300358z.
(27) Sussman, M. V.; Chin, L. Liquid Water in Frozen Tissue: Study by Nuclear Magnetic Resonance. *Science* **1966**, *151* (3708), 324-325. DOI: 10.1126/science.151.3708.324 (acccessed 2022/10/28).
(28) Volke, F.; Pampel, A.; Haensler, M.; Ullmann, G. Proton MAS NMR of a protein in a frozen aqueous solution. *Chemical Physics Letters* **1996**, *262* (3), 374-378. DOI: https://doi.org/10.1016/0009-2614(96)01062-7.
(29) Choi, M. J.; Briançon, S.; Andrieu, J.; Min, S. G.; Fessi, H. Effect of Freeze-Drying Process Conditions on the Stability of Nanoparticles. *Drying Technology* **2004**, *22* (1-2), 335-346. DOI: 10.1081/DRT-120028238.
(30) Feigon, J.; Denny, W. A.; Leupin, W.; Kearns, D. R. Interactions of antitumor drugs with natural DNA: proton NMR study of binding mode and kinetics. *Journal of Medicinal Chemistry* **1984**, *27* (4), 450-465. DOI: 10.1021/jm00370a007. Ackerman, J. J. H.; Soto, G. E.; Spees, W. M.; Zhu, Z.; Evelhoch, J. L. The NMR chemical shift pH measurement revisited: Analysis of error and modeling of a pH dependent reference. *Magnetic Resonance in Medicine* **1996**, *36* (5), 674-683, https://doi.org/10.1002/mrm.1910360505. DOI: https://doi.org/10.1002/mrm.1910360505 (acccessed 2022/11/02).
(31) Wishart, D. S.; Bigam, C. G.; Yao, J.; Abildgaard, F.; Dyson, H. J.; Oldfield, E.; Markley, J. L.; Sykes, B. D. 1H, 13C and 15N chemical shift referencing in biomolecular NMR. *Journal of Biomolecular NMR* **1995**, *6* (2), 135-140. DOI: 10.1007/BF00211777.
(32) Thorat, A. A.; Munjal, B.; Geders, T. W.; Suryanarayanan, R. Freezing-induced protein aggregation - Role of pH shift and potential mitigation strategies. *J Control Release* **2020**, *323*, 591-599. DOI: 10.1016/j.jconrel.2020.04.033.

https://doi.org/10.26434/chemrxiv-2023-mmxqx **ORCID:** https://orcid.org/0000-0001-5063-3218 Content not peer-reviewed by ChemRxiv. **License:** CC BY-NC-ND 4.0

(33) Green, A. A. The Preparation of Acetate and Phosphate Buffer Solutions of Known PH and Ionic Strength. *Journal of the American Chemical Society* **1933**, *55* (6), 2331-2336. DOI: 10.1021/ja01333a018.
(34) Hauptmann, A.; Podgorsek, K.; Kuzman, D.; Srcic, S.; Hoelzl, G.; Loerting, T. Impact of Buffer, Protein Concentration and Sucrose Addition on the Aggregation and Particle Formation during Freezing and Thawing. *Pharm Res* **2018**, *35* (5), 101. DOI: 10.1007/s11095-018-2378-5.
(35) Arsiccio, A.; Pisano, R. The Ice-Water Interface and Protein Stability: A Review. *J Pharm Sci* **2020**, *109* (7), 2116-2130. DOI: 10.1016/j.xphs.2020.03.022.
(36) Strambini, G. B.; Gonnelli, M. Protein Stability in Ice. *Biophysical Journal* **2007**, *92* (6), 2131-2138. DOI: https://doi.org/10.1529/biophysj.106.099531.
(37) Fahy, G. M.; MacFarlane, D. R.; Angell, C. A.; Meryman, H. T. Vitrification as an approach to cryopreservation. *Cryobiology* **1984**, *21* (4), 407-426. DOI: https://doi.org/10.1016/0011-2240(84)90079-8.
(38) Randolph, T. W. Phase Separation of Excipients during Lyophilization: Effects on Protein Stability. *Journal of Pharmaceutical Sciences* **1997**, *86* (11), 1198-1203. DOI: https://doi.org/10.1021/js970135b.
(39) Strambini, G. B.; Gabellieri, E. Proteins in frozen solutions: evidence of ice-induced partial unfolding. *Biophysical Journal* **1996**, *70* (2), 971-976. DOI: https://doi.org/10.1016/S0006-3495(96)79640-6.
(40) Setia, S.; Mainzer, H.; Washington, M. L.; Coil, G.; Snyder, R.; Weniger, B. G. Frequency and causes of vaccine wastage. *Vaccine* **2002**, *20* (7), 1148-1156. DOI: https://doi.org/10.1016/S0264-410X(01)00433-9.

https://doi.org/10.26434/chemrxiv-2023-mmxqx **ORCID:** https://orcid.org/0000-0001-5063-3218 Content not peer-reviewed by ChemRxiv. **License:** CC BY-NC-ND 4.0